

HYBRID EVALUATION METHOD OF BRIDGE BEARING CAPACITY

PENGZHEN LU^{1*}, SAID M. EASA², YING WU³, ZHENYI QI¹,
YIZHOU ZHUANG¹

¹*Zhejiang University of Technology, Hangzhou 310014, Zhejiang Province, China*

²*Department of Civil Engineering, Ryerson University,
Toronto, Ontario M5B 2K3, Canada*

³*Jiaying Nanhu University, Jiaying 314001, Zhejiang Province, China*

Received 19 March 2024; accepted 14 July 2024

Abstract. This study proposes a new method to assess the bearing capacity of similar bridges while avoiding the disadvantages of costly static loading tests. First, we present a detailed evaluation of the bearing capacity for a repaired pre-stressed concrete continuous-beam bridge following a ship collision. We have developed a finite element model, modified it, and combined with two other methods to evaluate its bearing capacity. The first method proposed is the bridge design code-based method, where the bearing capacity is assessed using specified design parameters. The second is the field test-based method, where the bearing capacity is evaluated using field tests combined with structural appearance observation. Considering the relative merits of these two methods, a new and improved method for bearing capacity evaluation is proposed and implemented by combining the design code, finite element model, and field loading tests. The innovation and contribution of this paper lie in obtaining modal parameters through a convenient dynamic load test to predict the static behaviour of the bridge structure based on the modified finite element model. Based on the dynamic test results, the static behaviour of the bridge, predicted

* Corresponding author. E-mail: pengzhenlu@zjut.edu.cn

Pengzhen LU (ORCID ID 0000-0003-4608-9648)

Said M. EASA (ORCID ID 0000-0003-0754-138X)

Copyright © 2024 The Author(s). Published by RTU Press

This is an Open Access article distributed under the terms of the Creative Commons Attribution License (<http://creativecommons.org/licenses/by/4.0/>), which permits unrestricted use, distribution, and reproduction in any medium, provided the original author and source are credited.

by the modified finite element analysis, and the appearance test data of the bridge structure, the bearing capacity of the bridge structure is evaluated.

Keywords: bearing capacity of bridge, dynamic and static loading, finite-element model, repair and strengthening.

Introduction

Highway bridges are the throat of the transportation network. Some bridges are inevitably exposed to all types of structural damage due to the natural aging of structures, increased vehicle loads, adverse environmental impacts, and the lack of maintenance and repair. The damage may also be caused by the mismanagement of human factors, ship collisions, and vehicle impacts. This damage reduces the bearing capacity and decreases the durability of bridge structures. As a result, the operating conditions do not meet the requirements of regulations, which may trigger bridge collapse or malfunction. Therefore, developing an easy, fast, economical, and reliable method to evaluate the bearing capacity of existing bridges, especially for damaged bridges, has become very important and urgent. The bearing capacity evaluation provides the theoretical basis for bridge repair-maintenance planning and a vital link to ensure the safety and smoothness of the transportation network. Since the load-bearing capacities of some existing bridges do not meet the requirements anymore, developing a proper evaluation method is essential.

According to the report from the American Federal Highway Administration, the total number of bridges in the United States is approximately 617 000, of which about 42 000 bridges have issues. By the end of 2020, the total number of structurally deficient bridges in the United Kingdom was 3105, which increased to 3211 by the end of 2021. The growth rate of structurally deficient bridges was 3.4% from 2019 to 2020 and 5% from 2020 to 2021. Structurally deficient bridges now represent approximately 4.5% of the total number of bridges in the United Kingdom. The total number of bridges in Japan is approximately 700 000, with over 33 000 bridges having issues. As of the end of 2023, the total number of highway bridges in China was 1.0793 million. Among the bridges in service, 40% have been in operation for over 20 years, and 30% of the bridges with technical grades three and four are in a suboptimal condition (Zhou and Zhang, 2019).

The statistics show that, at present, more than 40% of China's highway bridges have served longer than 20 years. Up to 30% of the bridges are working with distresses technically classified as grade III or IV, and more than 100 000 bridges are tagged as dangerous bridges.

Many existing bridges have deficient bearing capacity and require mitigating the risk of failure. How to accurately evaluate the bearing capacity of these bridges economically has become a hot topic in the study of bridge safety, reliability, and durability (Melchers, 2001). In particular, it has become urgent to detect and evaluate old bridges and bridges repaired after being impacted by ships to determine their actual performance states, including the actual bearing capacity and residual service life. This can help develop a reasonable and economical technical retrofitting design scheme for the bridges to improve their structural performance. This paper focuses on the quick and accurate bearing capacity evaluation method of existing bridges, based on the case study of a repaired bridge after a ship collision.

Ship-bridge collisions have been taking place all over the world (Sha et al., 2021). Between 1970 and 1974, there were 811 ship-bridge impacts in the United States. Statistically, within the 33 years from 1960 to 1993, the number of large bridges damaged by ships reached 29 in the world. During the period of 1959–1990, China also had more than 70 ship-bridge pier impacts in Nanjing, Jiujiang, Zhicheng, Wuhan, and other cities. The frequent ship collisions worldwide cause losses to bridge authorities and ship owners. Larsen (1993) published a guide on the interaction between traffic vessels and bridge structures. The author summarised the existing research of ship-bridge collisions and provided suggestions to promote future work. In an academic conference in Denmark, the participants discussed the problems in-depth and promoted an international study of ship-bridge collisions (Gluver and Olsen, 1998). The American Association of State Highway and Transportation Officials (AASHTO) guide aids bridge structural design under ship impact loads and is universally recognised worldwide (AASHTO, 1991).

At present, bridges are sometimes damaged by accidental loads, such as earthquakes (Xie and Yang, 2020), ship impacts, vehicle-bridge collisions and fire, etc. However, the urgent problem for bridge maintenance and maintenance defenders is whether the damaged bridge structure needs to be strengthened. What is its carrying capacity? It is necessary to make timely decisions and judgments on whether to continue traffic operations or stop operations, which is very important for the effective management and maintenance of bridges. The focus of this paper is to propose a hybrid evaluation and decision-making method for the performance of damaged bridge structures after the damage caused by earthquakes, car collisions, ship collisions and fire, etc. The emphasis is on the method of performance evaluation and decision-making of bridge structures, rather than the damage caused by loads on bridge structures. Wan et al. (2019) carried out a test and

Table 1. Comparison of existing bearing capacity evaluation methods for bridges

| Category | Evaluation Method | Features | Pros | Cons | References |
|----------|-------------------------|---|--|---|--------------------------|
| E | Empirical | Quantitative scoring system based on damage evaluation to structures | Simple, easy to use | Rough result, long cycle, limited application range | Kamiński and Bien (2013) |
| C | Design Code | Based on design code/specification and measured data | Straight forward, strong theory, and widely applied | less in-situ data, less accurate | Li (1996) |
| F | Loading Test | Based on static or dynamic loading test, the experimental results and theoretical analysis are compared | Objective, accurate, and direct | Large-scale, expensive, interrupt traffic, cause damage | Kovács et al. (2016) |
| A | Dynamic Parameter | Dynamic response is measured to reflect mechanical properties of bridge structure | Simple, reliable, advanced, does not affect traffic | Large error and complex computations | Bennati et al. (2016) |
| | AHP | Decomposing evaluation objectives into several levels, obtaining overall evaluation using initial weights and bridge test results | Transforms qualitative problems into quantitative ones, scientific and effective | Immature theory, not widely applied | Nieto et al. (2019) |
| | Reliability Theory | Using failure probability or reliability index to judge the structure's safety level | Considers uncertainties of load and force resistance | Minimal consideration and not mature theory | Kim et al. (2013) |
| | Dynamic Reliability | Determining bearing capacity using actual and target time-varying reliability indices | Considers various factors, evaluation results are reliable | Theory is not mature | Jamali et al. (2019) |
| | Calibration Coefficient | bearing capacity is determined based on the calibration coefficient | Scientific and perfect, with accurate results | Not widely applied, lack of referable bridge types | Liu et al. (2018) |
| E-A | Expert System | Evaluation using computer systems with the equivalent level of expert knowledge and experience | Fast and simple | Subjective, only qualitative descriptive results | Papayianni et al. (2016) |

| | | | | |
|-----------------------------|--|---|---|----------------------|
| Vibration Test | Selecting correction parameters, modifying FE model using vibration test, and evaluate bearing capacity using structural analysis | Reliable results | No technical breakthrough and lack of practical formula | Sudath (2015) |
| Optical Fibre Sensing | Taking passing load as test load, using optical fibre sensor in construction to collect the strain and evaluate bearing capacity | Simple and quick, real-time evaluation | High requirements, not widely applied | Wu et al. (2017) |
| Modal Analysis | Using traditional power spectrum, identifying bridge modal parameters, and evaluating bridge conditions | No traffic interruption, directly reflect operating condition | Additional mass impact, not mature | Ma et al. (2019) |
| Fuzzy Closeness | Combining fuzzy theory with engineering evaluation to obtain fuzzy evaluation results, considering proximity of related fuzzy grades to evaluate bridge bearing capacity | Avoiding the failure of evaluation results, reflecting the truth and evaluating quickly | Not mature, narrow range of applications | Liu et al. (2021) |
| Digital Image | Processing the cracking-captured images using Matlab to provide a reference for bridge bearing capacity assessment | High efficiency and good application prospect | High requirements for equipment and complex analysis | Monique (2021) |
| Quasi-static Influence Line | Combining finite element model correction technology and rapid evaluation method of field quasi-static continuous measurement | Small consumption and quick assessment | Limited research results, not widely applied | Liang & Xiong (2020) |
| F-A-C | Combining design code, field testing and FEA | Relatively fast/inexpensive, reasonably accurate | Complex data of field test and design code | This paper |

^a AHP = analytical hierarchy process, FE = finite element.

^b A = analytical, C = design code, E = empirical, F = field, E-F = empirical-field, E-A = empirical-analytical, F-A = field-analytical, and F-A-C = field-analytical-design code.

Pengzhen Lu,
Said M. Easa,
Ying Wu,
Zhenyi Qi,
Yizhou Zhuang

Hybrid Evaluation
Method of Bridge
Bearing Capacity

conducted a finite element (FE) simulation analysis of ship-bridge pier collision to evaluate the anti-ship collision performance of a reinforced concrete bridge pier. Gholipour et al. (2018) studied the ship impact on the reinforced concrete column dynamic response and failure behaviour under the transverse impact using numerical simulation. Based on the theory of ship-bridge collision, Liu et al. (2014) used the FEA software ANSYS to develop a bridge calculation model and then to analyse ship-bridge collisions. Little research has been conducted on the evaluation of the bearing capacity of old or repaired bridges.

Several methods to evaluate the bridge bearing capacity have been developed, ranging from simple methods, such as appearance observation and design code, to more complex methods, such as analytical hierarchy process (AHP), fuzzy evaluation, and neural network. Their features are summarised and compared in Table 1. Among more famous studies, Martinelli et al. (2018) carried out a load test and numerical study on an arch bridge built in the 14th century in Lecco city, Italy. They evaluated its bearing capacity based on the field load test results. Using the AHP method combined with the grey correlation theory, Xu et al. (2015) proposed a more accurate and reliable evaluation method by reducing the unobvious influences from the minor factors in the evaluation process. Omar et al. (2017) proposed an evaluation method for reinforced concrete bridge decks. Sobhani and Masoodi (2023) proposed a differential quadrature technique for frequencies of the coupled circular arch–arch beam bridge system, and appointed to discover the dynamic behaviour related to one of the most applicable systems used in engineering, namely coupled beam bridge system, concrete bridge decks based on fuzzy mathematics, while Weinstein et al. (2018) used the artificial neural network to identify bridge damage. Combining the AHP, Delphi method, and Cloud model, Peng et al. (2019) proposed a group decision-making method based on cloud clustering, involving experts' score, risk probability and risk loss.

The comparison of various bridge assessment methods in Table 1 shows that similarities and differences coexist. For example, the bridge code method has a solid theoretical basis and has been widely used. However, it is inappropriate to directly implement the method to assess the bearing capacity because the parameters in design and evaluation are different. The design code is developed with no consideration of the influence of force resistance over time, and, therefore, the reliability calculation model of the proposed structure is static. However, materials such as concrete and reinforcement slowly degenerate with time, and the load will vary with time. The time-varying reliability calculation model must be established by considering the influence of the time factor. The field-loading test method is the most direct and reliable in bridge

bearing capacity evaluation, but its cost is so enormous that the method is challenging to be popular. Besides, this method may cause severe structural damage and affect normal traffic. This is particularly true for existing bridges that lack essential raw data. Therefore, there is a need for a systematic, inexpensive, fast and accurate method for the bearing capacity evaluation to help guide bridge repair and management.

This paper proposes a new method for the bearing capacity evaluation that combines the design code, FE analysis, and field-loading test. The method is described in the context of a case study involving the Wanjiang Bridge in China after a ship impact. The next sections describe the evaluation process of bearing capacity and the FE modelling. The following sections present the design-code and field-test evaluation methods, followed by a summary of applying the proposed hybrid method for evaluating other bridges and the conclusions.

1. Evaluation process

Before describing the process of bearing capacity evaluation of the repaired bridge, it is helpful to describe the bridge and the collision before repair briefly. The Wanjiang Bridge is a strut-framed pre-stressed concrete continuous girder bridge crossing over the Dongguan waterway, Guangdong Province, China. The bridge has separate dual box girders with constant depth (Figure 1). The deck is 12-m wide (two 4.5-m vehicle lanes and two 1.5-m walkways) with design load Vehicle-15, Tractor Trailer-80 and crowd load 3 KPa (MTPRC, 2012). The bridge was built in 1976 and was the first pre-stressed concrete continuous girder bridge built by China's incremental launching construction method.

The bridge was impacted by a ship in 2006, and the three strut-frames on one side of Pier 5, nearer to the bridge mid-span, were severely damaged (Figure 1). Some concrete members in the supporting brackets fall into the river, leading to apparent changes in the bridge structural and mechanical behaviour. After the collision, the municipality immediately asked relevant agencies to inspect and mitigate the damage, and the bridge was subsequently repaired and restored to its typical performance.

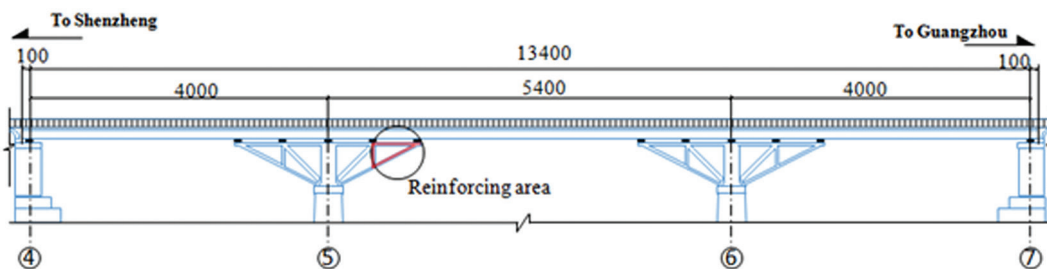
The bearing capacity of pre-stressed reinforced concrete bridges is influenced by various factors, including material quality, construction quality, maintenance level, external forces, design rationality, and time-related aspects. Comprehensive data collection, detailed investigation of the current situation, and the preparation of structural diagrams are necessary during inspections. Key areas of focus during inspections

include the bridge deck profile, concrete strength and carbonation, pre-stress loss, rebar configuration, and corrosion. It is essential to ensure the safety of the inspection process, handle data scientifically, and provide targeted recommendations to accurately assess the bridge bearing capacity.

Following a ship collision with the Wanjiang Bridge, the management department conducted a comprehensive inspection, including visual and structural examinations. The inspection revealed four main issues with the bridge: (1) Severe damage to the reinforced concrete diagonal bracing on the west side of the pier due to the impact of the vessel; (2) damage to the bridge expansion joint, leading to the accumulation of silt and direct entry of rainwater into the pier top; (3) water accumulation inside the box girder of the 4th to 5th axis beam, causing local infiltration; (4) lack of protective piers for the bridge piers to minimize the risk of accidental vessel impact.

During the pre-stress inspection of the bridge, it was observed that the concrete in the pre-stressed tendon anchorage zones did not exhibit cracking, there were no longitudinal cracks on the concrete surface along the pre-stressed tendons, and there was no evidence of rebar corrosion.

(a) Geometry of the north half of the bridge



(b) Cross section

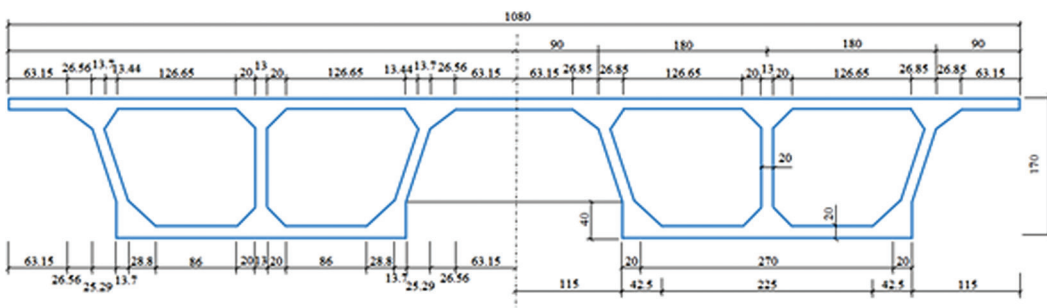


Figure 1. Overall layout and cross section of the Wanjiang Bridge (unit: cm)

The bearing capacity was evaluated using FE simulation, design code, and field loading test. The proposed hybrid evaluation method of bearing capacity is shown in Figure 2. First, FE software was used to simulate and analyse the mechanical performance of the bridge after the ship's impact. The software accurately described the continuous beam geometric shape and spatial characteristics, and provided the mechanical performance at the control sections before the repair and after the repair of the impacted bridge. Then, the static and dynamic loading tests were carried out based on the results from the simulation analysis. The bending moment envelope and deformations at the main sections, under the vehicle and crowd load, were calculated using the dynamic loading test. Note that the data from the loading test were used to modify the initially established FE model. Since the initial finite element model is usually established according to the design data in the simulation analysis of the bridge structure, to make the finite element model truly reflect the actual stress situation of the bridge structure, it is often necessary to revise the initial finite element model. There are many methods for revising the finite element model, such as modifying material properties, structural geometry, and boundary conditions (Lan et al., 2023; Lu et al., 2023). In this paper, however, the initial finite element model of the bridge structure is modified by using modal parameters such as frequency obtained from the dynamic load test of the bridge. The concrete steps are as follows: First, the initial finite element model is established to obtain the frequency and vibration mode of the bridge structure. Then the measured frequency and vibration mode of the bridge structure are obtained by dynamic load test. The error between the measured value and the initial theoretical value of the finite element is compared. The response surface model is established, the optimal parameters are calculated, and the predicted stiffness value of the bridge structure is obtained by using the measured frequency. The initial finite element model is modified by using the predicted stiffness values. Then, the modified FE model is used to evaluate the bearing capacity of the bridge structure. After the rapid evaluation of the damaged bridge structure performance by the method proposed in this paper, the basic performance of the bridge structure is determined, and whether the bridge needs further static load test or reinforcement is determined. If it is necessary to further understand the actual bearing capacity of the damaged bridge structure, a static load test is needed, and the test results of the static load test are compared with those of the method in this paper for verification. If there is any error, the modified finite element model can be further modified to form a more accurate baseline finite element model. Therefore, the bearing capacity of the post-impact bridge was evaluated by comparing the results from the

simulation and loading tests, including the calibration coefficients of the strain and deflection, natural frequency, and damping ratio. Finally, the bridge structural resistance and load effect were modified based on the loading test results, and the bearing capacity was re-evaluated using the bridge design code.

2. Finite element modelling

2.1. Background

The relationship between the element-node force and the node displacement is essential in the FE modelling. In the FE analysis, if the whole structure has n elements, the force-displacement relation has n equations as follows:

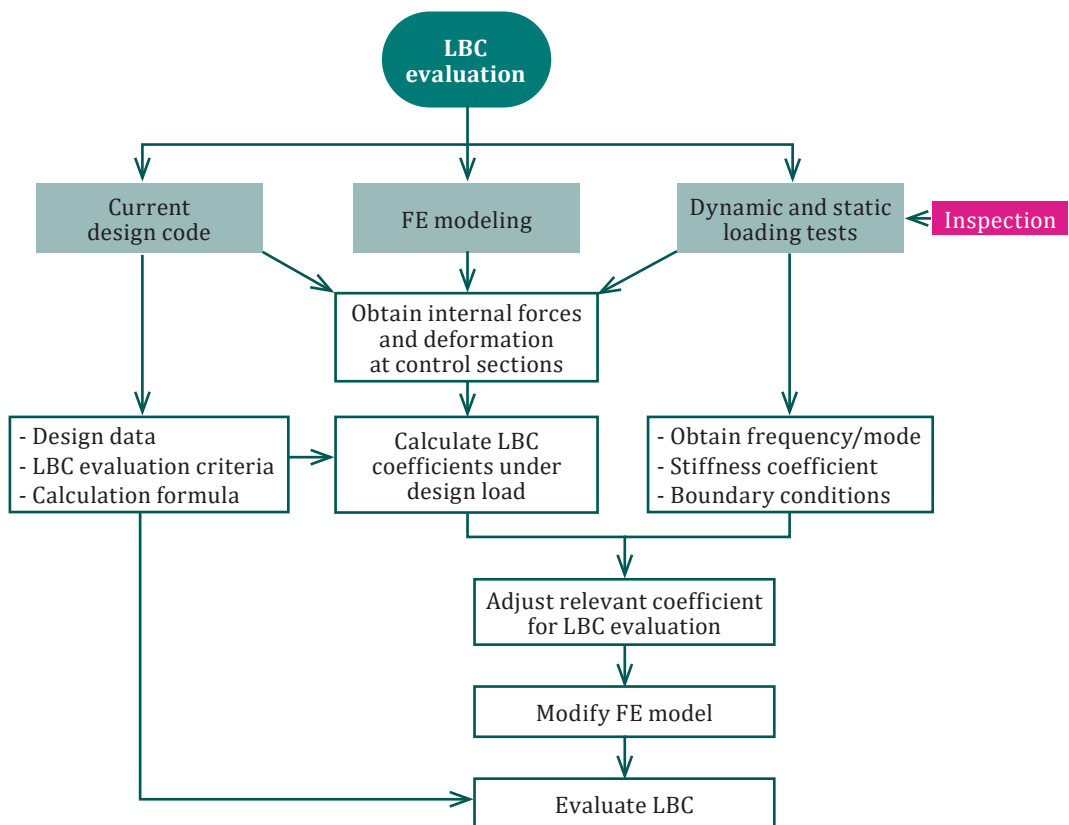


Figure 2. The proposed field-analytical-design code method of bearing capacity evaluation of an existing bridge

$$\begin{Bmatrix} f_1 \\ f_2 \\ f_3 \\ \vdots \\ f_n \end{Bmatrix} = \begin{bmatrix} k_1 & 0 & 0 & 0 & 0 \\ 0 & k_2 & 0 & 0 & 0 \\ 0 & 0 & \cdot & 0 & 0 \\ 0 & 0 & 0 & \cdot & 0 \\ 0 & 0 & 0 & 0 & k_n \end{bmatrix} \begin{Bmatrix} s_1 \\ s_1 \\ s_3 \\ \vdots \\ s_n \end{Bmatrix}, \quad (1)$$

where f_1 to f_n are elements of the internal forces, k_1 to k_n are elements of the stiffness matrix, and s_1 to s_n are displacement elements.

Since the stiffness matrix is diagonal, Equation (1) can be written in matrix form as

$$f = k_s s, \quad (2)$$

where k_s is a diagonal stiffness matrix.

Denoting the integral stiffness matrix of the structure as K , the node equilibrium equation of the entire structure becomes

$$F = K\delta, \quad (3)$$

where F is a node-load vector and δ is a node displacement vector of the structure.

Equation (3) is the solution for the initial FE of the structure, which is usually modified to improve the solution. The structure is then discretized based on the FE theory, where a limited number of easily analysed elements connected by a finite number of nodes are used.

2.2. Developing initial FE model

The FE model of the whole bridge was developed based on the size and material characteristics of the Wanjiang Bridge using the general FE software ANSYS. The bridge piers, abutments, and supporting brackets were simulated by Solid45 elements, while Beam188 elements simulated the pile foundation. The mesh size was 20 cm, and a total of 20 512 units were used. Reinforcement density was 7800 kg/m³, elastic modulus was 2E11 MPa, Poisson's ratio was 0.3, and the yield strength was 300 MPa. Concrete density was 2500 kg/m³, elastic modulus was 3E10 MPa, Poisson's ratio was 0.167, ultimate tensile strength was 1.43 MPa, ultimate compressive strength was 14.3 MPa. The time step was 0.05 s of the bridge structure simulation analysis. The full-bridge FE representation is shown in Figure 3. Based on the FE model, the internal force and deformation of the bridge structure at the measurement sections under the design load were calculated to determine the loading size and mode in the field-loading tests. The process of developing the FE model was as follows:

1. Based on the characteristics and material properties of the superstructure, substructure, and boundary conditions of the Wanjiang Bridge, the mechanical model for the stress analysis of the bridge structure was established;
2. A suitable element for each bridge component was selected using the mechanical model and the analytical properties of the bridge;
3. The corresponding elements and their material properties were assigned to different structure components, where the concrete parameters were determined using the design code (MTPRC, 2018);
4. Based on the structural stress characteristics of the three-span continuous beam bridge, the boundary conditions were applied as one fixed hinge support and other movable rolling supports, with all simulated by 3D Solid45 elements;
5. Phased testing truckloads were then applied according to the design load-cases for the static loading test;
6. The FE model was then solved, and the results were obtained.

(a) Finite element model of space bar of full bridge

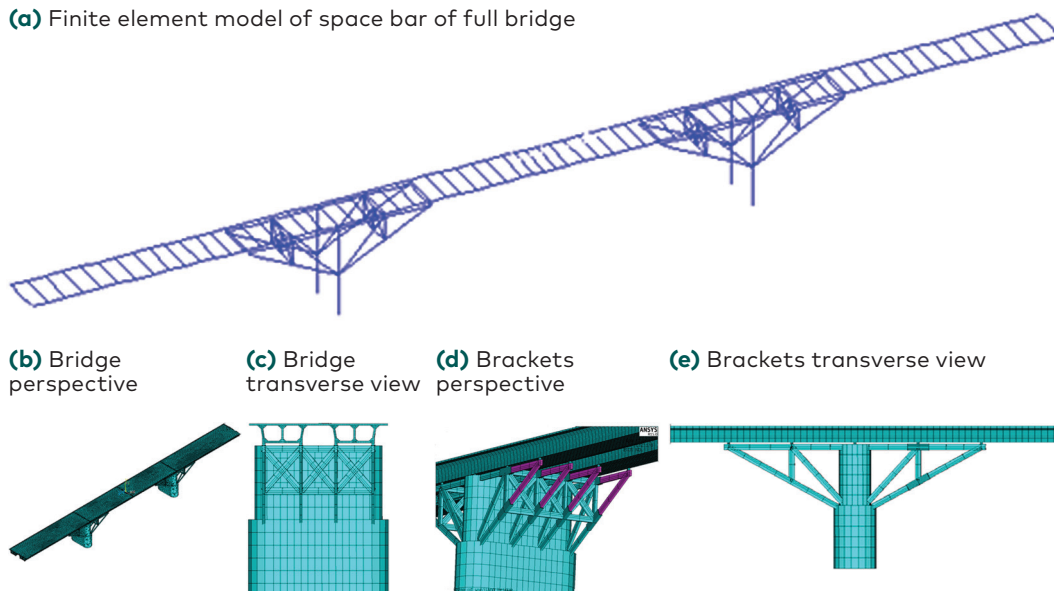


Figure 3. FE modelling of the meshed elements of the repaired Wanjiang Bridge

2.3. Static loading test

It was required to maintain the relationship between the structural test load and the corresponding displacement and prevent accidental damage to the structure. Therefore, the static loading mode was monotonically run to the maximum load and instantly unloaded to zero. The purpose was to determine the loading positions and conditions that satisfy the test-load efficiency using the fewest number of loading vehicles. At the same time, it was essential to simplify the loading cases, shorten the testing time, and adequately merge the loading cases under the premise of satisfying the test-load efficiency. Each load case was based on a specific inspection project while considering other inspection items. According to the Chinese standard (MTPRC, 2011), the maximum load of a static loading test is determined based on the loading efficiency η , as explained later.

2.4. Modified FE model

When building the finite element model of the bridge structure, there is inevitably a difference between the built finite element model and the real situation of the structure. The characteristic information types currently used for model correction are mainly divided into static information, dynamic information, and combined dynamic and static information to establish an accurate finite element model. However, using the static loading test to obtain static information has disadvantages such as high cost, obstruction to traffic, and damage to the bridge structure.

Bridge structure finite element model correction methods can be roughly divided into matrix type and design-parameter type. The matrix model modification method needs to rely on the mass and stiffness matrix, which is unsuitable for large-scale bridge structures. It is not easy to apply to actual structures because the modified results lose clear physical meaning. A more reasonable method is to directly modify the design parameters, including materials, cross-sectional shape, and geometric dimensions of the structure. This method has a clear physical meaning and is currently the most suitable modification method for engineering applications. Therefore, in this paper, design data, existing historical data, and similar bridge material performance indicators combined with the dynamic load test were used to modify the FE model and evaluate the bridge bearing capacity.

Since the mechanical properties of the repaired Wanjiang Bridge were unknown, the developed FE model was modified to achieve the most realistic FE results, guarantee the field test safety, and avoid the

structural damage caused by the test. The FE model adjustment involved a probabilistic optimisation procedure that consisted of the following steps:

1. Start with the initial FE modelling;
2. Select the parameter to be adjusted, such as the material elastic modulus or the sectional parameters. In this paper, the elastic modulus was selected as the adjusted parameter using the actual conditions of the Wanjiang Bridge;
3. Generate a certain number of learning samples using the Uniform Experimental Design Method (maximizing the efficiency of sample selection);
4. Obtain the structural frequency by solving the FE model and generate the training learning samples;
5. Construct the response surface model (RSM), using the training samples to approximate the optimal solution by making the constructed mathematical RSM close to the respective FE response surface;
6. Obtain the field-test structural frequency and develop a regression surface to determine the parameters of the modified FE model.

The preceding adjustment method mainly involved the RSM, which was used to solve the optimisation problem with multiple design variables. Its basic idea is to approximate the implicit functional relationship between the objective function and the design variables by constructing the RSM (a polynomial) with an explicit form. Then, the optimization results can be obtained by solving the RSM under the corresponding constraints. Mathematically, a specific set of samples is needed in the construction of the RSM. For variables, a complete two-order (including cross-terms) response surface approximation function is given by

$$\hat{y} = \hat{f}(x_1, x_2, \dots, x_k) = \beta_0 + \sum_{i=1}^k \beta_i x_i + \sum_{i=1}^k \beta_{ii} x_i^2 + \sum_{i=1}^k \sum_{j=1}^k \beta_{ij} x_i x_j, \quad (4)$$

where \hat{y} is a response surface function of the optimization target, x_i ($i = 1, 2, \dots, k$) – input variables of the response surface models (design parameters of bridge structure), and β_0 , β_i , β_{ii} , and β_{ij} – undetermined coefficients.

The total number of undetermined coefficients for an RSM of k input variables is $n_t = (k + 1)(k + 2)/2$. The values of these coefficients are determined using sample tests. In this paper, the Uniform Experimental

Design Method was used for experimental design. This method provides an accurate response surface using fewer test points. The coefficient matrix of the RSM was obtained by the least square method and was used to establish the RSM. The accuracy of the RSM was evaluated using the complex correlation coefficient $R^2(p)$. The response surface regression analysis can be written as an optimization model as follows:

$$\text{Min} \|R(p)\|_2^2, R(p) = \{f_E\} - \{f_A\} \quad (5)$$

subject to

$$VLB \leq p \leq VUB, \quad (6)$$

where p - design parameters, $\{f_E\}$, $\{f_A\}$ - characteristic quantities of the analysis and the experiment, respectively, VLB , VUB - lower and upper ranges of the design space, respectively, and $R(p)$ - residual.

According to the modified FE model, the internal forces and static deformation behaviours at the control sections of the bridge structure were analysed. Figure 4(a) shows the FEA results after the ship collision and before the repair, and Figure 4(b) shows the FEA results after the reinforcement and repair. All those results from the FEA, dynamic characteristics and static field test before and after repair confirmed that the new support bracket met the design requirements. The structure was in the elastic working range during the test, and the measured index met the design code requirements. The dynamic loading test data showed that the general stiffness of the bridge after the repair was higher than that before repair, and the performance was good.

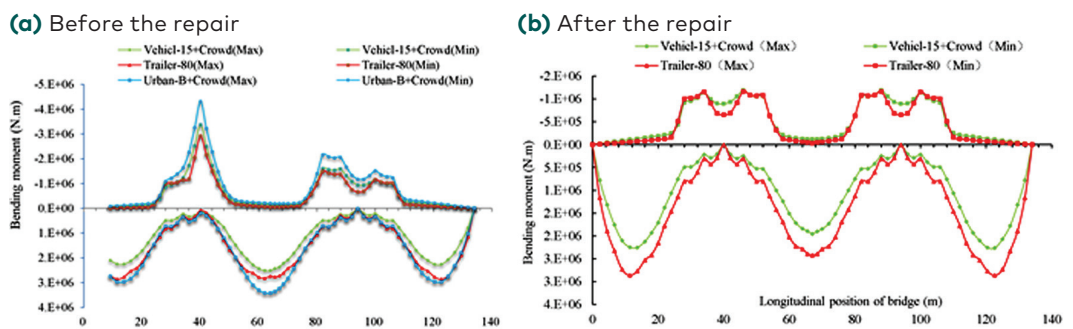


Figure 4. Bending moment diagram of the Wanjiang Bridge before and after the repair

3. Design code-based evaluation

Using the Chinese bridge design code, *Specification for Inspection and Evaluation of Load-bearing Capacity of Highway Bridges* (MTPRC, 2011) and considering the defective conditions in material strength and natural vibration frequency, the resistance of the Wanjiang Bridge was revised. This was accomplished using an appearance survey, the bearing capacity deterioration coefficients, and the sectional reduction coefficients of the concrete and reinforcement.

3.1. Bearing capacity related coefficients

Checking coefficient of bearing capacity, Z_1 .

The assessment scale of the checking coefficient of bearing capacity is given by

$$D = \sum \alpha_j D_j, \quad (7)$$

where D – an overall assessment scale for Z_1 , α_j – weight of item j , and D_j – a scale of item j .

Three items were used in Equation (7): defective condition (2, 0.4), material strength (1, 0.3), and natural vibration frequency (2, 0.3), where the first and second numbers of each item refer to its weight and scale, respectively. Based on Equation (7), D is 1.7. Then, from the design code, the checking coefficient Z_1 is determined using linear interpolation as 1.11.

Deterioration coefficient of bearing capacity, ζ_e .

The assessment scale of the deterioration coefficient is given by

$$E = \sum \alpha_j E_j \quad (8)$$

where E – an overall assessment scale for ζ_e and E_j – a scale of item j .

Seven items were used in Equation (8). Their weights and scales are shown in Table 2. Based on Equation (8), E is 1.64. Using this design code value, the deterioration coefficient of bearing capacity ζ_e is determined by linear interpolation as 0.06.

Table 2. Assessment scale E on the deterioration coefficient of bearing capacity^a

| No. | Detection index | Weight, α_j | Item scale, E_j |
|-----|---|--------------------|-------------------|
| 1 | Concrete apparent defect | 0.32 | 2 |
| 2 | Reinforcement natural potential | 0.11 | 1 |
| 3 | Concrete resistivity | 0.05 | 1 |
| 4 | Concrete carbonation depth | 0.20 | 2 |
| 5 | Concrete cover depth | 0.12 | 2 |
| 6 | Chloride (Cl) | 0.15 | 1 |
| 7 | Structural concrete strength estimation | 0.05 | 1 |

^aAccording to the design code, a scale of three items (concrete resistivity, concrete carbonation depth, and chloride) should be taken as 1 when the process need not be evaluated.

Sectional reduction coefficient of concrete ζ_c .

The assessment scale of this coefficient is given by

$$R = \sum \alpha_j R_j, \quad (9)$$

where R – an overall assessment scale for ζ_c and R_j – a scale of item j .

Three items were used in Equation (9): material weathering (0.1, 2), concrete carbonation (0.35, 2), and physical and chemical damage (0.55, 2), where the first and second numbers of each item refer to its weight and scale, respectively. Based on Equation (9), R is 2. Then, from the design code, the coefficient ζ_s is determined by linear interpolation as 0.98. According to the simulation of the Wanjiang Bridge after repair, the failure section of the bridge was located at 0.3 L in a side span between Piers 4 and 5, controlled by positive bending moment. Therefore, the load and resistance at this section was selected for the bearing capacity checking.

Sectional reduction coefficient of reinforcement, ζ_s

There are a few cracks in the bridge, and the width of the cracks is less than the maximum permissible limit. Using the design code, this coefficient ζ_s was determined as 0.98.

3.2. Effect of load combination

The load effect is obtained according to the most unfavourable combination of various loading cases. The bending moment diagram of the repaired bridge under the combined loads of Vehicle-15, Tractor-80, Urban-B, and the crowd load is illustrated in Figure 4. After the repair,

the internal control force in a single box girder under the dead and live loads was established. As noted, the positive bending moment of the single box girder is maximum only under Urban-B and crowd load. At the failure section, the positive bending moment in a single box girder under Urban-B, crowd load, and dead load are $Q_K = 2.63 \times 10^6$ N·m, $L_K = 0.33 \times 10^6$ N·m, and $G_K = 8.56 \times 10^6$ N·m, respectively. Then, the combined loading effect is expressed as

$$S = 1.2G_K + 1.4Q_K + 0.75 \times 1.4L_K, \quad (10)$$

where S – a combined load effect, G_k – a standard value of the dead load effect, Q_k – a standard value of the vehicle load effect, and L_k – a standard value of the crowd load effect.

Under the composition action of the dead and live loads, a single box girder's maximum positive bending moment $S = 14.30 \times 10^3$ kN·m.

Revised resistance.

The resistance of the bridge was revised based on the four coefficients previously described as follows:

$$R = R(f_d, \zeta_c \alpha_{dc}, \zeta_s \alpha_{ds}) Z_1 (1 - \zeta_e), \quad (11)$$

where $R(\cdot)$ – a function of the resistance effect, f_d – design strength of the metrical, α_{dc} – a geometrical parameter of the component concrete, α_{ds} – a geometrical parameter of the component steel, Z_1 – a load capacity checking coefficient, ζ_e – a load capacity deterioration coefficient, ζ_c – a sectional reduction coefficient of the reinforced concrete, and ζ_s – a sectional reduction coefficient of the steel.

The initial resistance effect at the failure section was 17.96×10^6 N·m, whereas the resistance effect after the revision was equal to 17.31×10^6 N·m.

3.3. Checking of ultimate bearing capacity

The bearing capacity for the bridge structure was checked first by examining the defective bridge conditions, checking bridge material property and status parameters, and investigating actual operating load conditions to determine the partial checking coefficients. Then, based on those coefficients, the bridge bearing capacity under the ultimate limit state and the allowable value under the service limit state were adjusted. Finally, the predicted effect was compared with the modified resistance (or allowable value) to determine whether the predicted results met the requirements. Using the preceding method, the ultimate bridge bearing capacity was calculated. The results showed that the rate of the most

unfavourable load effect on bearing capacity of a single box girder was 0.83, indicating that the bearing capacity had a surplus and satisfied the design load requirements (Vehicle-15, Tractor-trailer-80, and Urban-B).

4. Field loading-based evaluation

Actual static and dynamic loading tests of the repaired bridge were conducted to evaluate actual bearing capacity and judge the bridge safety after repair. To evaluate the performance of the new supporting frame, the sections in the upper and lower chords of the new bracket and the box girder section supported by the new bracket were selected as test locations around Pier 5.

4.1. Static loading test

Loading procedure. In this test, four heavy vehicles were used as the test loads and were divided into three loading cases and one unloading case, as follows: Case 1 (two trucks are loaded symmetrically), Case 2 (one truck is loaded on a lane by the side of the walkway), Case 3 (one truck is loaded on a lane near to central median), and Case 4 (unloading case, where all vehicles on the bridge deck are removed). In Cases 1–3, the rear axle was 1.5 m from the mid-span. After being weighed, the loading trucks park outside the bridge, and the weight difference between the actual and weighted values was not more than 1 ton. The total weight of the test vehicle ranged from 32 560 kg to 33 320 kg. When all the work arrangements were in place, the reading of each test was adjusted to zero for the first no-loading reading. Then, the test was carried out in a graded loading procedure. The test sections (box girder and support frame at Pier 5) and the loading positions are shown in Figure 5.

Once every single vehicle was moved to the specified area, a stable 15-minute interval was needed before the first reading was recorded. The second reading was recorded using a 10-minute interval. If the difference between the two readings was less than 10%, the structural performance change was considered stable. In the loading process, one of the following conditions should stop the loading (the reason was subsequently analysed): (1) the control point value of the stress or the internal force exceeds the calculated value and meets or exceeds the corresponding values required by the provisional safety conditions; (2) the control point deflection, such as vertical deflection, exceeds the allowable design value, or (3) the structural components are subjected

to mechanical or local damage, which affects the bridge bearing capacity and typical service performance.

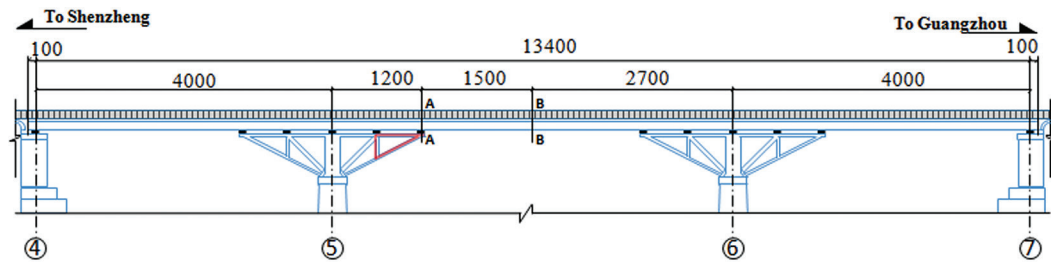
Loading efficiency. In the static loading test, the maximum test load is determined based on the loading efficiency, which is given by (MTPRC, 2012).

$$\eta = \frac{S_t}{S_d \times \delta}, \quad (12)$$

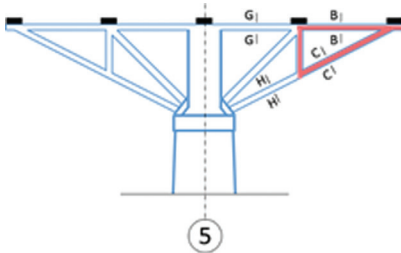
where η – loading efficiency, S_t , S_d – the calculated value of the deformation or the internal force at the measurement sections under the test load and the design standard load, respectively, and δ – a design impact coefficient (0.80–1.05), assumed 1.0 in this test. The range of η is 0.95–1.05.

To illustrate, the axial force calculated values in each control section of Box Girders 1 and 2 are shown in Table 3. The internal loading efficiency for the bending moment and the axial force under each test case are shown in Table 4. As noted, the maximum negative bending moment loading efficiency of the newly added support-frame box girder Section A-A at Pier 5 is 0.887. The maximum positive bending moment loading efficiency of the mid-span section ($L/2$) is 1.019. The maximum axial tension loading efficiency of the newly added support frame Section

(a) Box girder



(b) Loading locations for Cases 1-3



(c) Supporting frame at Pier 5

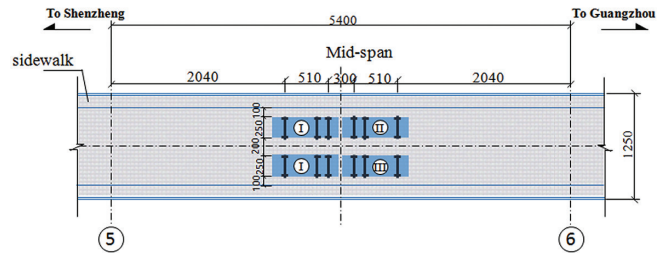


Figure 5. Static loading test sections (unit: cm)

B-B is 0.874. Finally, the maximum axial stress loading efficiency of the newly added support frame Section C-C is 0.866. All loading efficiencies satisfy the provisions of the design code, which requires a loading efficiency of (0.8 to 1.0) for the heaving loading test and (0.5 to 0.8) for the light loading test (CIHS, 1982).

Measurement scheme and procedure. The arrangement for deformation measurement points is shown in Figure 6(a). As noted, the

Table 3. Axial force in a single frame under test load (Right Frame at Pier 5)^a

| Location (Section) | Axial Force (N) at Box Girder 1 (East side) | | | Axial Force (N) at Box Girder 2 (West side) | | |
|--------------------------|---|--------|--------|---|--------|--------|
| | Case 1 | Case 2 | Case 3 | Case 1 | Case 2 | Case 3 |
| Side upper chord (B-B) | 1.54 | 2.00 | 2.77 | 1.54 | 2.31 | 2.77 |
| Centre upper chord (G-G) | 2.15 | 2.70 | 3.77 | 2.15 | 3.22 | 3.77 |
| Side lower chord (C-C) | -1.73 | -2.25 | -3.11 | -1.73 | -2.60 | -3.11 |
| Centre lower chord (H-H) | -1.77 | -2.29 | -3.16 | -1.77 | -2.63 | -3.16 |

^a Multiplying each value by 10⁵.

Table 4. Bending moment and axial force loading efficiency under the test loads, %

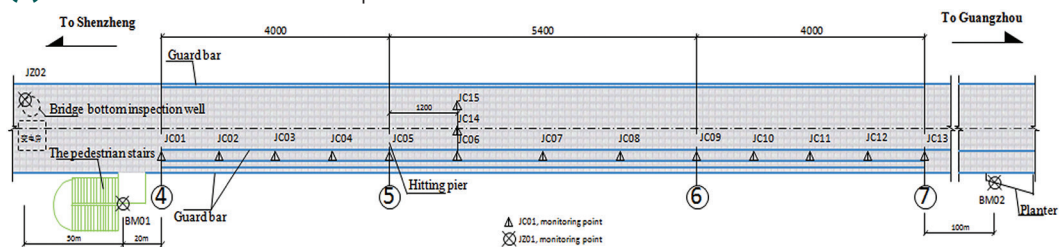
| Location (Section) | Box Girder 1 (East side) | | | Box Girder 2 (West side) | | |
|---|--------------------------|--------|--------|--------------------------|--------|--------|
| | Case 1 | Case 2 | Case 3 | Case 1 | Case 2 | Case 3 |
| (a) Bending Moment (Piers 5 and 6) | | | | | | |
| Top of Pier 5 | 15.4 | 24.2 | 25.5 | 15.4 | 17.9 | 25.5 |
| Bracket centre support | 44.6 | 67.5 | 80.9 | 44.6 | 62.2 | 80.9 |
| Bracket side support | 43.7 | 73.9 | 88.7 | 43.7 | 63.4 | 88.7 |
| L/4 (A-A) | 26.7 | 58.8 | 72.1 | 26.7 | 42.6 | 72.1 |
| L/2 (A-A) | 51.0 | 86.3 | 101.9 | 51.0 | 71.1 | 101.9 |
| 3L/4 (A-A) | 45.4 | 65.6 | 72.2 | 45.4 | 55.6 | 72.2 |
| Bracket side support | 45.5 | 76.1 | 88.7 | 45.5 | 62.7 | 88.7 |
| Bracket centre support | 36.2 | 65.6 | 80.9 | 36.2 | 55.0 | 80.9 |
| (b) Axial Force (Pier 5 Right Frame) | | | | | | |
| Side upper chord (B-B) | 48.6 | 63.1 | 87.4 | 48.6 | 72.9 | 87.4 |
| Centre upper chord (G-G) | 42.3 | 53.1 | 74.2 | 42.3 | 63.4 | 74.2 |
| Side lower chord (C-C) | 48.2 | 62.7 | 86.6 | 48.2 | 72.4 | 86.6 |
| Centre lower chord (H-H) | 48.4 | 62.6 | 86.3 | 48.4 | 72.9 | 86.3 |

measurements were taken at 15 points that were fixed on the bridge deck pavement with 8-cm expansion bolts. The vertical deformation was measured using levelling equipment with Ni005A-precision level (ZEISS, German) and a levelling accuracy of 0.1 mm.

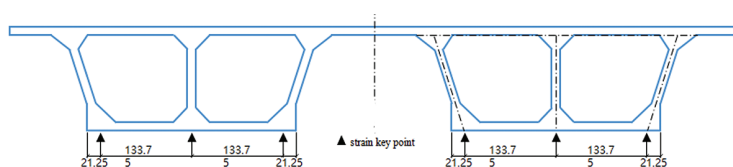
The strain measurement points were set at: (1) the box girder Section A-A supported by the newly added support frame; (2) Sections B-B and G-G of the upper chord, and (3) Sections C-C and H-H of the lower chord near the mid-span of the bridge at Pier 5. Figure 6(b) shows that Section A-A has six strain measurement points. Figure 6(c) shows that Sections G-G and H-H have one strain measurement point on the top and the two side edges, respectively, while Sections B-B and C-C have one strain measurement point on the top, the bottom, and the two side edges. Thus, this static loading test was arranged with 62 strain measurement points. The measured data included the strains at all loading cases and the residual strains after unloading. The data collector was TDS-303 made by TML, Japan.

Analysis of static test results. The measured and calculated deflections under loading Case 3 and unloading Case 4 are shown in Table 5. As noted, the maximum measured elastic deflection is -8.9 mm, compared with a calculated value of -9.4 mm, giving a ratio of 0.95, which lies within the range required by the design code (0.7 to 1.05). In addition, the allowable vertical deflection for the pre-stressed concrete girders equals $f=L/600$, where L is the maximum span, m, (MTPRC, 2011),

(a) Deformation measurement points



(b) Section A-A



(c) B-B and G-G

(d) C-C and H-H

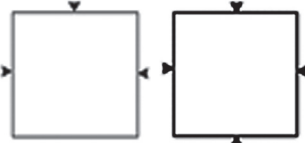


Figure 6. Arrangement of deformation and strain measurement points (unit: cm)

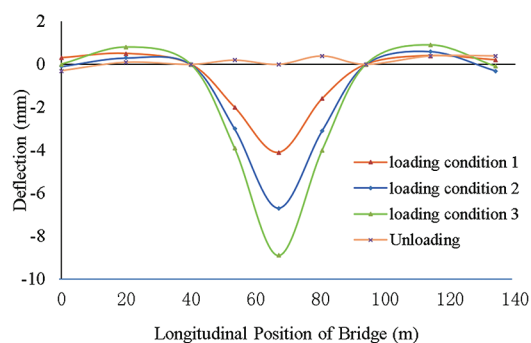
giving $f=54000/600=90$ mm. Therefore, the maximum measured deflection is less than the allowable value and satisfies the design code. The measured and calculated deflections for different loading cases are shown in Figure 7. The measured and calculated strains at the measurement points in Section A-A and the bracket supporting frame sections under Case 3 are shown in Table 5. As noted, the maximum measured elastic strain is $-45 \mu\epsilon$ at point C3 of Section C-C, while its calculated elastic strain is $-46 \mu\epsilon$, giving a ratio of 0.94. This ratio, which ranges from 0.7 to 1.05, satisfies the requirements of the standards (CIHS, 1982).

Table 5. Deflections under loading Case 3 and unloading Case 4

| Location | Measured ^a , mm | Calculated ^a , mm | Unloading, mm | S_e/S_{stat} |
|---------------|----------------------------|------------------------------|---------------|----------------|
| Top of Pier 4 | 0.0 | 0.0 | -0.3 | - |
| $L/2$ | 0.8 | 0.8 | 0.1 | 0.88 |
| Top of Pier 5 | 0.0 | 0.0 | 0.0 | - |
| $L/4$ | -3.9 | -4.5 | 0.2 | 0.91 |
| $L/2$ | -8.9 | -9.4 | 0.0 | 0.95 |
| $3L/4$ | -4.0 | -4.5 | 0.4 | 0.98 |
| Top of Pier 6 | 0.0 | 0.0 | 0.0 | - |
| $L/2$ | 0.9 | 0.8 | 0.0 | 0.63 |
| Top of Pier 7 | -0.1 | 0 | 0.4 | - |

^a The positive values indicate upheaval. S_e = Measured value of the maximum elastic deflection. S_{stat} = Theoretical value of the max elastic deflection.

(a) Measured deflections



(b) Calculated deflections

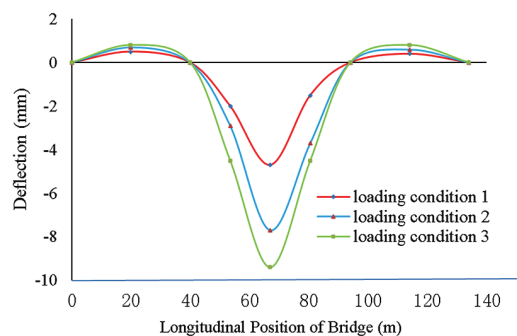


Figure 7. The measured and calculated deflections for different loading cases

Table 6. Strains on section A-A and bracket supporting frame under loading
Case 3 and unloading Case 4

| Measurement Points | | Measured, mm | Calculated, mm | Unloading, mm | S_e/S_{stat} |
|--|--------------------|--------------|----------------|---------------|----------------|
| (a) Cross Section A-A | | | | | |
| | A1 | -21 | -28 | 1 | 0.82 |
| | A2 | -28 | -28 | 2 | 0.82 |
| | A3 | -15 | -28 | 4 | 0.82 |
| | A1-A3 ^a | -21 | -28 | 2 | 0.82 |
| | A4 | -23 | -28 | 0 | 0.99 |
| | A5 | -31 | -28 | -4 | 0.99 |
| | A6 | -29 | -28 | -3 | 0.99 |
| | A4-A6 ^a | -28 | -28 | -2 | 0.99 |
| (b) Bracket supporting frame sections | | | | | |
| B-B | B1 | 28 | 37 | 0 | 0.76 |
| | B2 | 25 | 37 | -1 | 0.70 |
| | B3 | 28 | 37 | -1 | 0.78 |
| | B4 | 24 | 37 | -3 | 0.73 |
| C-C | C1 | -42 | -46 | -2 | 0.87 |
| | C2 | -44 | -46 | 1 | 0.98 |
| | C3 | -45 | -46 | -1 | 0.96 |
| | C4 | -41 | -46 | -1 | 0.87 |
| G-G | G1 | 41 | 65 | -2 | 0.66 |
| | G2 | 42 | 65 | -2 | 0.68 |
| | G3 | 43 | 65 | -1 | 0.68 |
| H-H | H1 | -40 | -51 | 0 | 0.78 |
| | H2 | -41 | -51 | 2 | 0.84 |
| | H3 | -43 | -51 | 2 | 0.88 |
| | H4 | -41 | -51 | 1 | 0.82 |

^a Average values were used.

Regarding the residual deformation and strains, the maximum measured elastic deflection is -8.9 mm at $L/2$, and the residual deformation is 0.0 (Table 4), giving a ratio of 0.0. In addition, the maximum measured elastic strain is $-45 \mu\epsilon$, and the residual strain is $-1 \mu\epsilon$ (Table 6), giving a ratio of 0.02. Therefore, both residual deformation and strain satisfy the maximum ratio of 0.2 (MTPRC, 2011).

4.2. Dynamic loading test

The purpose of the dynamic loading test was to test the self-vibration characteristics and the forced vibration characteristics of the bridge structures using ground pulsation, truck jumping, and truck running (Figure 8). The ground pulsation test was carried out in the natural environment with no loads on the bridge. Then, the truck-jumping test was performed using a loaded truck weighing about 100 kN and having its rear-wheel go through a bumper about 15-cm high, which forced the detected bridge to vibrate. Finally, the truck running test was implemented using a loaded truck weighing about 100 kN and running at 20 km/h and 40 km/h to force the bridge to vibrate.

In the dynamic loading test, the sensor measuring points were arranged along one bridge side, located at $L/2$, $L/4$, and $3L/4$ in the spans between Piers 4 and 5, and Piers 5 and 6. The measured acceleration spectra of the repaired bridge at $L/4$ points using ground pulsation, truck running and truck jumping are shown in Figure 9. The analysis of the dynamic measurement data showed that the first-order self-vibration frequency of the bridge was 4.11 Hz and the damping ratio



Figure 8. Details of dynamic loading test

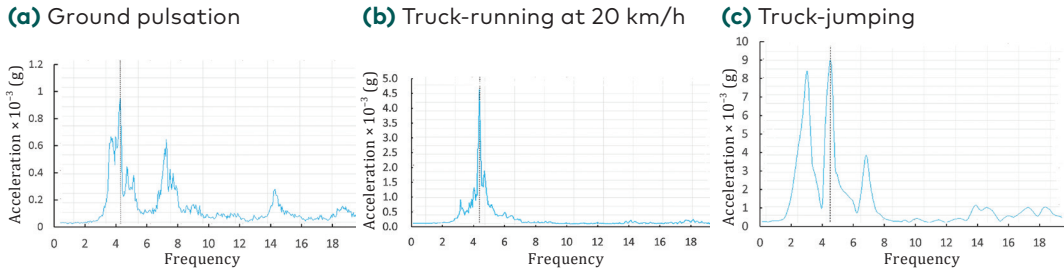
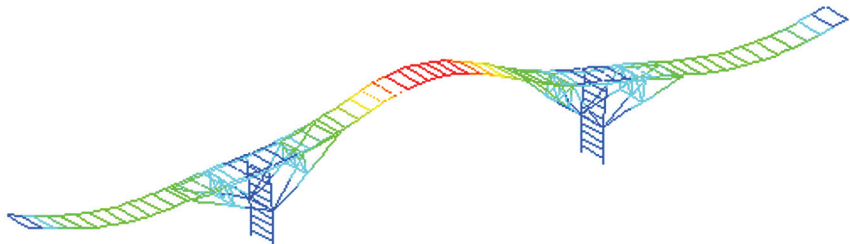
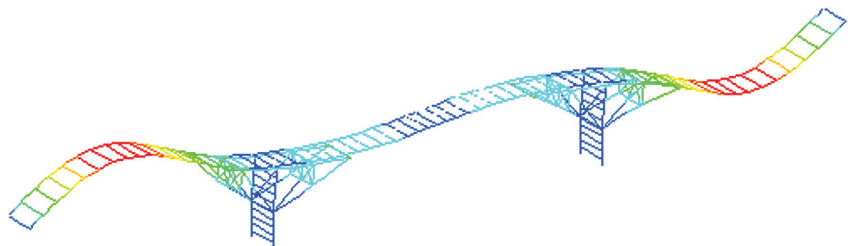


Figure 9. Frequency-acceleration spectrum diagram at mid-span section of the main girder

(a) Mid-span symmetrical vertical bending (3.12 Hz)



(b) Side-span vertical bending (3.67 Hz)



(c) Mid-span asymmetrical bending (7.21 Hz)

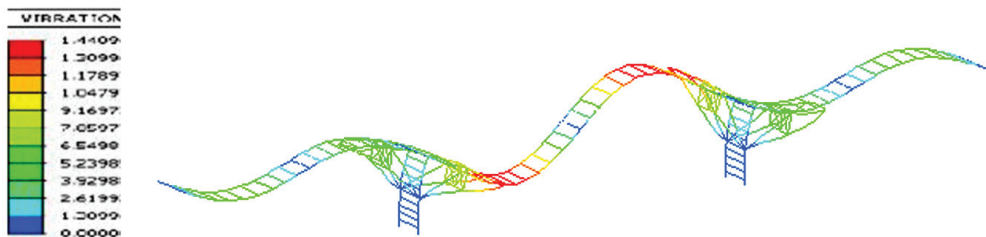


Figure 10. Mode shapes and calculated natural frequencies of the repaired Wanjiang Bridge

was 2.8–4.3% after the repair. In comparison, the measured first-order natural frequency of the bridge was 3.32 Hz before the reinforcement. This 23.7% increase indicates that the global rigidity of the repaired structure had substantially improved. The calculated natural vibration frequency and the mode shapes of the repaired bridge are shown in Figure 10. After the strengthening, the theoretically calculated first-order frequency of the bridge was 3.12 Hz. The measured frequency is greater than the theoretically calculated value, indicating that the actual stiffness of the bridge after strengthening was greater and the driving performance was better.

4.3. Discussion of loading test results

In the static loading test, the measured loading efficiency, bridge deflection, residual deformation, and strain of the newly added supporting bracket satisfied the design code provisions (MTPRC, 2018). This indicates that the bearing capacity and service performance of the bridge and the newly added bracket frame meet the requirements. Furthermore, the dynamic loading test showed that the first-order natural vibration frequency of the repaired bridge increased by 19%, indicating that the rigidity improvement of the bridge after the repair was substantial and the driving performance was good. Therefore, its bearing capacity can satisfy the design load requirements (Vehicle-15, Tractor-trailer-80, and Urban-B). Based on these results, it was concluded that the performance of the Wanjiang Bridge after repair had been brought to normal, and the repair method used was rational and valid.

The evaluation method of the design code theoretically relies on the code formulas. The resistance formula modified by the itemized checking coefficient was used to check the bearing capacity of the bridge. This method is suitable for bridges with field investigations or loading test data and a detailed evaluation of their defective conditions. The process of evaluation based on the field loading test allows for the direct determination of the stress level at specific parts of the bridge. It effectively helps avoid hidden defects in bridge inspection, thus leading to more accurate and reliable evaluation results. After checking and calculating the bearing capacity, the loading test data were again used to evaluate the bearing capacity and bridge performance to verify the accuracy of the analytical results.

5. Evaluating bearing capacity of other bridges

The proposed hybrid method can be applied to similar bridges (old or repaired) to evaluate their load bearing capacities, as follows: (1) building a FE model of the bridge using the structural analysis software; (2) using the bridge design data and the bearing capacity design-code criteria, calculating the coefficients related to bearing capacity evaluation of the bridge under the design load. In addition, performing the dynamic loading test to obtain the bridge frequency and vibration mode shape, from which the corresponding stiffness coefficient and boundary conditions are determined; (3) based on the design specifications, determining the internal force and deformation at the bridge control sections using the FE method and the dynamic loading test; (4) through field investigation of the bridge structure, obtaining the main parameters for bridge evaluation, including geometric morphological parameters, variations of dead load and material strength, corrosion of steel reinforcement, chloride ion content in concrete, and carbonization of concrete; (5) combining these parameters of the single-bridge structure with self-vibration frequencies of other bridge structures obtained using dynamic loading tests and evaluating the bearing capacity of other existing bridges using the checking coefficient, sectional reduction coefficient, and bearing capacity deterioration coefficient, based on similar bridge previous assessment experience, and (6) starting the bearing capacity assessment by modifying the FE model, assessing the bearing capacity based on the design code, analysing the base frequency and vibration mode shapes from the dynamic loading test, and analysing bridge checking data.

Concluding remarks

This paper presented a hybrid method for evaluating the bearing capacity of bridges that integrated three evaluation methods (supplemented by field inspection): design code, FE modelling, and field-loading tests (static and dynamic). The method was illustrated using the repaired Wanjiang Bridge, a strut-framed pre-stressed concrete continuous girder bridge located in China. Based on this study, the following conclusions were made:

1. The design code-based method for evaluating bridge bearing capacity was theoretical and mainly relied on the design code standards. This method was combined with the FE modelling and field loading tests. Considering the defective conditions, actual material strength, and natural vibration frequency of the bridge, the resistance of

the bridge was revised by adopting several coefficients, including bearing capacity checking coefficient, bearing capacity deterioration coefficient, sectional reduction coefficient of the concrete and reduction coefficient of the reinforcement. Subsequently, the ultimate bearing capacity of the bridge at the control section under the most unfavourable load conditions was verified.

2. The evaluation method based on the modified FE model was comprehensive and reasonable. The method used the evaluation information obtained from the loading test, reflected the bridge actual working conditions, and helped evaluate the safety of its key sections and residual bearing capacity. Furthermore, the method can simulate the possible damage in bridge operation and predict its ability to resist damage.
3. The loading test data were used to verify the accuracy of the design code-based results. As a result, the research showed that the performance of the repaired Wanjiang Bridge after the collision had been brought to normal, and its bearing capacity satisfied the level of design load (Vehicle-15, Tractor trailer-80, or Urban-B) that the repair method was rational and valid. Namely, in order to evaluate the actual carrying capacity of the restored Wanjiang Bridge, the management unit carried out field tests of static load and dynamic load on the repaired Wanjiang Bridge. In this way, the static and dynamic load test results of repaired Bridges can be used to verify the method proposed in this paper. The deflection or strain measured by static load test in the field was compared with the predicted finite element value, and the bearing capacity was verified based on the predicted deflection and strain value. According to the comments of the reviewers, we revised it.
4. The code-based method of assessing the bearing capacity of bridges has a solid theoretical basis and has been widely used in practice. However, it was not ideal to directly follow this method because its predicted results might substantially vary from actual results. To address this issue, the design criteria, the safety factor, the structural damage, and the selection of the structural analysis method were modified based on the loading-test results of a single bridge. Then, the results of the single bridge combined with the bearing capacity code-based evaluation can be used to assess the bearing capacity of other similar bridges. This approach saved substantial loading-test costs and provided a better understanding of bearing capacity and bridge performance.
5. The bearing capacity evaluation was the basis for bridge repair and maintenance and was an essential part of bridge management. Therefore, mastering the basic characteristics of each assessment

method and understanding its advantages and limitations were required for carrying out bridge assessment. Based on this understanding, the advantages of various methods can be combined to achieve efficient, accurate, economical, and reliable hybrid bearing capacity assessment methods to improve the evaluation process of existing bridges. The method presented in this paper represents such a hybrid method.

6. Bridge evaluation was a relatively new field. Research in this field is vital for improving bridge evaluation, reducing bridge strengthening and replacement costs, and meeting the increasing transportation requirements. This paper presented a hybrid method for bearing capacity assessment of bridges based on loading test and bridge code, combined with the FE analysis. The method was illustrated using a case study on a single bridge loading test to obtain the information to modify the difference in the evaluation and design of load, resistance, and structural analysis. The proposed evaluation method represents a valuable tool for bearing capacity evaluation of similar bridges repaired after ship collisions. Furthermore, the findings of the study have proven valuable for future maintenance and management of the repaired bridge.

Data Availability Statement

All data, models, or code that support the findings of this study are available from the corresponding author upon reasonable request.

Acknowledgments & grants

The authors gratefully acknowledge the financial support provided by the Science and Technology Project of Zhejiang Provincial Department of Transportation (Grant No. 2018010, 2019H17 and 2019H14), the Scientific Research Fund of Zhejiang Provincial Education Department (Grant No. Y202250418), the Science and Technology Agency of Zhejiang Province (Grant No. LTGG23E080006), Jiaxing Science and Technology Bureau of China under Grant (2023AY11020), the National Natural Science Foundation of China (52208217), the Science Foundation of China (Postdoctoral Grant No. 2016M600352), and Zhejiang Key Laboratory of Civil Engineering Structures & Disaster Prevention and Mitigation Technology. This project has been supported by the Engineering Research Centre of the Ministry of Education for Renewable Energy Infrastructure Construction Technology.

REFERENCES

- AASHTO. (1991). *Guide specification and commentary for vessel collision design of highway bridges*. American Association of State Highways and Transportation Officials, Washington, D. C.
- Bennati, S., Colonna, D., and Valvo, P. S. (2016). Evaluation of the increased load bearing capacity of steel beams strengthened with prestressed FRP laminates. *Frattura ed Integrità Strutturale*, 10(38), 377–391. <https://doi.org/10.3221/IGF-ESIS.38.47>
- CIHS. (1982). *Test method of long-span concrete bridge*. People's Communications Press, Beijing, China (YC4-4 /1978) China Institute of Highway Science (in Chinese).
- Gholipour, G., Zhang, C., and Mousavi, A. A. (2018). Effects of axial load on nonlinear response of RC columns subjected to lateral impact load: Ship-pier collision. *Engineering Failure Analysis*, 91, 397–418. <https://doi.org/10.1016/j.engfailanal.2018.04.055>
- Gluver, H., and Olsen, D. (1998). *Ship collision analysis. Proceedings of the International Symposium on Advances in Ship Collision Analysis*, Routledge, Copenhagen, Denmark.
- Jamali, S., Chan, T., Nguyen, A., and Thambiratnam, D. (2019). Reliability-based load-carrying capacity assessment of bridges using structural health monitoring and nonlinear analysis. *Structural Health Monitoring*, 18(1), 20–34. <https://doi.org/10.1177/1475921718808462>
- Kamiński, T., and Bień, J. (2013). Application of kinematic method and FEM in analysis of ultimate load bearing capacity of damaged masonry arch bridges. *Procedia Engineering*, 57, 524–32. <https://doi.org/10.1016/j.proeng.2013.04.067>
- Kim, H. J., Kim, H. K., and Park, J. Y. (2013). Reliability-based evaluation of load carrying capacity for a composite box girder bridge. *KSCE Journal of Civil Engineering*, 17, 575–583. <https://doi.org/10.1007/s12205-013-0603-7>
- Kovács, N., Kövesdi, B., Dunai, L., and Takács, B. (2016). Loading test of the Rákóczi Danube Bridge in Budapest. *Procedia Engineering*, 156, 191–198. <https://doi.org/10.1016/j.proeng.2016.08.286>
- Lan, Y., Lin, W., and Zhang, Y. (2023). Bridge frequency identification using multiple sensor responses of an ordinary vehicle. *International Journal of Structural Stability and Dynamics*, 23(5), Article 2350056. <https://doi.org/10.1142/S0219455423500566>
- Larsen, O. D. (1993). Ship collision with bridges: The interaction between vessel traffic and bridge structures. *International Association for Bridge and Structural Engineering*, 4, 119–131. <https://doi.org/10.2749/sed004>
- Li, Y. D. (1996). Evaluation of bridge load-carrying capacity based on design code. *Journal of Bridge Construction*, 2, 61–63 (in Chinese).
- Lu, P., Li, D., Wu, Y., Chen, Y., and Wang, J. (2023). Static behavior prediction of concrete truss arch bridge based on dynamic test data and Bayesian inference. *International Journal of Structural Stability and Dynamics*, 24(9), Article 2450095. <https://doi.org/10.1142/S0219455424500950>

- Liang, Y. Z., and Xiong, F. (2020). Measurement-based bearing capacity evaluation for small and medium span bridges. *Measurement*, 149, Article 106938. <https://doi.org/10.1016/j.measurement.2019.106938>
- Liu, H., Li, B., Sun, Y. Q., Dou, X. Z., Zhang, Y. F., and Fan, X. H. (2021). Safety evaluation of large-size transportation bridges based on combination weighting fuzzy comprehensive evaluation method. *IOP Conference Series: Earth and Environmental Science*, 787(1), Article 012194. <https://doi.org/10.1088/1755-1315/787/1/012194>
- Liu, K., Yang, G., and Yang, K. (2014). Research and analysis of ship-bridge collision. *Applied Mechanics and Materials*, 638–640, 973–976. <https://doi.org/10.4028/www.scientific.net/AMM.638-640.973>
- Liu, X. L., Zhang, X. M., and Wang, Y. D. (2018). A rapid detection method for bridges based on impact coefficient of standard bumping. *Mathematical Problems in Eng.*, 2018, 1–14. <https://doi.org/10.1155/2018/9195289>
- Lu, P. Z., Pan, J. P., Hong, T., Li, D. G., and Chen, Y. R. (2020). Prediction method of bridge static deformation based on dynamic test. *Structural Concrete*, 21(6), 2533–2548. <https://doi.org/10.1002/suco.202000016>
- Ma, Q. L., Zhou, J. T., Ullah, S., and Wang, Q. (2019). Operational modal analysis of rigid frame bridge with data from navigation satellite system measurements. *Cluster Computing*, 22, 5535–5545. <https://doi.org/10.1007/s10586-017-1360-z>
- Martinelli, P., Galli, A., Braazzetti, L., Colombo, M., Felicetti, R., and Previtali, M. (2018). Bearing capacity assessment of a 14th-century arch bridge in Lecco (Italy). *International Journal of Architectural Heritage*, 12(2), 237–256. <https://doi.org/10.1080/15583058.2017.1399482>
- Melchers, R. E. (2001). Assessment of existing structures approaches and research needs. *Journal of Structural Engineering*, 127(4), 406–411. [https://doi.org/10.1061/\(ASCE\)0733-9445\(2001\)127:4\(406\)](https://doi.org/10.1061/(ASCE)0733-9445(2001)127:4(406))
- MTPRC. (2011). *Specification for inspection and evaluation of the load-bearing capacity of highway bridges* (JTG/T)21-2011). Ministry of Transportation of the People's Republic of China People's Communications Press, Beijing, China (in Chinese).
- MTPRC. (2012). *Code for the design of highway reinforced concrete and prestressed concrete bridges and culverts* (JTG D62-2012), Ministry of Transportation of the People's Republic of China People's Communications Press, Beijing, China (in Chinese).
- MTPRC. (2018). *Code for the design of highway reinforced concrete and prestressed concrete bridges and culverts* (JTG 3362-2018), Ministry of Transportation of the People's Republic of China People's Communications Press, Beijing, China (in Chinese).
- Monique, H. H. (2021). *Bridge load rating and evaluation using digital image measurements* (Final Report 03/18/2019 – 12/18/2021). Center for Integrated Asset Management for Multimodal Transportation Infrastructure Systems, University of Delaware. <https://rosap.nrl.bts.gov/view/dot/68361>
- Nieto, C. C., Shan, Y. W., Lewis, P., and Hartell, J. A. (2019). Bridge maintenance prioritization using analytic hierarchy process and fusion tables. *Automation in Construction*, 101, 99–110. <https://doi.org/10.1016/j.autcon.2019.01.016>

- Omar, T., Nehdi, M. L., and Zayed, T. (2017). Integrated condition rating model for reinforced concrete bridge decks. *Journal of Performance of Constructed Facilities*, 31(5), Article 04017090. [https://doi.org/10.1061/\(ASCE\)CF.1943-5509.0001084](https://doi.org/10.1061/(ASCE)CF.1943-5509.0001084)
- Papayianni, I., Papanikolaou, V. K., Andreopoulos, T. D., and Glykofrydis, D. (2016). Assessment of the bearing capacity of an old concrete bridge. *Structural Faults & Repair Conference*, Edinburgh. https://www.researchgate.net/publication/309668873_Assessment_of_the_bearing_capacity_of_an_old_concrete_bridge
- Peng, K. K. (2019). Risk evaluation for bridge engineering based on cloud-clustering group decision method. *Journal of Performance of Constructed Facilities*, 33(1), Article 04018105. [https://doi.org/10.1061/\(ASCE\)CF.1943-5509.0001255](https://doi.org/10.1061/(ASCE)CF.1943-5509.0001255)
- Sha, Y., Amdahl, J., and Drum C. (2021). Numerical and analytical studies of ship deckhouse impact with steel and RC bridge girders. *Engineering Structures*, 234, Article 111868. <https://doi.org/10.1016/j.engstruct.2021.111868>
- Sobhani, E., and Masoodi, A. R. (2023). Differential quadrature technique for frequencies of the coupled circular arch-arch beam bridge system. *Mechanics of Advanced Materials and Structures*, 30(4), 770–781. <https://doi.org/10.1080/15376494.2021.2023920>
- Sudath, C. S. (2015). Vibration measurement-based simple technique for damage detection of truss bridges: A case study. *Case Studies in Engineering Failure Analysis*, 4, 50–58. <https://doi.org/10.1016/j.csefa.2015.08.001>
- Wan, Y. L., Zhu, L., and Fang, H. (2019). Experimental testing and numerical simulations of ship impact on axially loaded reinforced concrete piers. *International Journal of Impact Engineering*, 125, 246–262. <https://doi.org/10.1016/j.ijimpeng.2018.11.016>
- Weinstein, J. C., Sanayei, M., and Brenner, B. R. (2018). Bridge damage identification using artificial neural networks. *Journal of Bridge Engineering*, 23(11), Article 04018084. [https://doi.org/10.1061/\(ASCE\)BE.1943-5592.0001302](https://doi.org/10.1061/(ASCE)BE.1943-5592.0001302)
- Wu, B. T., Wu, G., Lu, H. X., and Feng, D. C. (2017). Stiffness monitoring and damage assessment of bridges under moving vehicular loads using spatially distributed optical fiber sensors. *Smart Materials and Structures*, 26(3), Article 035058. <https://doi.org/10.1088/1361-665X/aa5c6f>
- Xie X., Yang T. Y. (2020). Performance evaluation of Chinese high-speed railway bridges under seismic loads. *International Journal of Structural Stability and Dynamics*, 20(5), Article 2050066. <https://doi.org/10.1142/S0219455420500662>
- Xu, Y. F., Wang, H. L., and Zhang, L.Q. (2015). Research on safety assessment method for bridge structure based on variable weight synthesis method. *Perspectives in Science*, 7, 200–203. <https://doi.org/10.1016/j.pisc.2015.11.033>
- Zhou, X., Zhang, X. (2019). Thoughts on the development of bridge technology in China. *Engineering*, 5(6), 1120–1130. <https://doi.org/10.1016/j.eng.2019.10.001>